This article was downloaded by: [Siauliu University Library]
On: 17 February 2013, At: 07:14
Publisher: Taylor & Francis
Informa Ltd Registered in England and Wales Registered Number: 1072954 Registered office: Mortimer House, 37-41 Mortimer Street, London W1T 3JH, UK

Advanced Composite Materials
Publication details, including instructions for authors and subscription information:
http://www.tandfonline.com/loi/tacm20

Estimation of interfacial properties from hysteretic energy loss in unidirectional ceramic matrix composites

J. P. Solti , D. D. Robertson & S. Mall
Version of record first published: 02 Apr 2012.

To cite this article: J. P. Solti , D. D. Robertson & S. Mall (2000): Estimation of interfacial properties from hysteretic energy loss in unidirectional ceramic matrix composites, Advanced Composite Materials, 9:3, 161-173

To link to this article: http://dx.doi.org/10.1163/15685510051033322

PLEASE SCROLL DOWN FOR ARTICLE

Full terms and conditions of use: http://www.tandfonline.com/page/terms-and-conditions

This article may be used for research, teaching, and private study purposes. Any substantial or systematic reproduction, redistribution, reselling, loan, sub-licensing, systematic supply, or distribution in any form to anyone is expressly forbidden.

The publisher does not give any warranty express or implied or make any representation that the contents will be complete or accurate or up to date. The accuracy of any instructions, formulae, and drug doses should be independently verified with primary sources. The publisher shall not be liable for any loss, actions, claims, proceedings, demand, or costs or damages whatsoever or howsoever caused arising directly or indirectly in connection with or arising out of the use of this material.

Adv. Composite Mater., Vol. 9, No. 3, pp. 161–173 (2000)
© VSP 2000.

Downloaded by [Siauliu University Library] at 07:14 17 February 2013

Estimation of interfacial properties from hysteretic energy loss in unidirectional ceramic matrix composites

J. P. SOLTI [1], D. D. ROBERTSON [2] and S. MALL [3,*]

[1] *United States Air Force Academy, HQ USAFA/DFEM, Colorado 80840, USA*
[2] *Air Force Corrosion Program Office, WL/MLS-OL, Robins AFB, GA 31098, USA*
[3] *Air Force Research Laboratory, AFIT/ENY, 2950 P Street, Building 640, Wright-Patterson Air Force Base, Ohio 45433, USA*

Received 10 May 1999; accepted 30 December 1999

Abstract—When ceramic matrix composites are subjected to fatigue loading levels sufficient to initiate microstructural damage to the constituents, the mechanical response of the laminate, e.g. the residual strength, stiffness and life of the composite, is governed by the physical state of the fiber/matrix interface. During loading, the chemical bonds, which develop between fiber and matrix during processing, are broken. This 'debonding' results in a significant decline in load transfer between the two constituents and leads to a measurable increase in laminate compliance.

With continued cyclic loading, the interface debonds grow in length which further degenerates the composite strength. Moreover, within the debonded regions, frictional sliding between the fiber and matrix is permitted and leads to surface wear of the constituents [1]. Ultimately, the progression of this damage mode leads to a further decline in the interfacial shear stress and load transfer between the constituents.

Knowledge of the progression of both damage mechanisms, debonding and the reduction in interfacial shear strength, is critical to characterize ceramic composites since these mechanisms govern, in large part, the degradation in laminate properties. Unfortunately, experimental observation of these kinds of damage is not an easy task. However, attempts to measure these properties experimentally using single fiber and microcomposite tests have been conducted [2, 3]. Moreover, several techniques for estimating interfacial properties computationally using various models have been presented in the literature [4–8]. As in this study, several micromechanics models use hysteresis measurements to gain insight into the state of the fiber/matrix interface [4–6, 8]. The authors use the hysteresis data for a myriad of purposes ranging from the derivation of empirical constants to validation of simplified failure criterion. The current study is unique in that assumptions are *not* made regarding either the failure of the interface (debonding), nor the associated degradation in shear resistance during fatigue. The present study attempts to infer a logical progression of both mechanisms without specific failure criteria. Rather, the analysis is a 'what must they be' comparison between the experimental measurements of hysteretic energy loss within a given fatigue cycle and the numerical predictions from the one-dimensional shear-lag analysis. The strength of the model and its application as presented herein resides in its simplicity allowing the validated approach to be incorporated into

[*] To whom correspondence should be addressed. E-mail: shankar.mall@afit.af.mil

more rigorous micromechanics models which more accurately model the instantaneous state of stress within the laminate as has been the evolution of the early shear-lag models.

Keywords: Ceramics matrix composites; fatigue; shear-lag analysis; modeling; hysteretic energy.

Downloaded by [Siauliu University Library] at 07:14 17 February 2013

1. INTRODUCTION

Ceramic Matrix Composites (CMCs) exhibit a remarkable increase in strain-to-failure as compared with their monolithic counterparts [9]. The incorporation of the fiber-reinforcement phase into the brittle matrix leads to microstructural interactions that reduce the propensity for catastrophic failure of the laminate. The degree of toughening exhibited by CMCs is, in large part, a function of the fiber/matrix interfacial properties, specifically the frictional shear resistance along debonded regions and the bond strength within fully constrained (bonded) areas [10, 11]. As such, determination of the instantaneous interfacial properties is critical for effective modeling of these materials.

As these inherently brittle materials are loaded, several forms of constituent damage develop (Fig. 1). Since the strain-to-failure of the matrix tends to be less than the strain-to-failure of the fibers, one primary damage mechanisms is the development of cracks ('matrix cracks') which traverse the matrix material perpendicular to the loading axis. In addition, large crack-tip stresses associated with these matrix cracks can initiate debonding along the fiber/matrix interface [12]. Finally, the fibers themselves are subject to fracture. These damages become more prevalent with monotonic loading or continuous loading, i.e. fatigue; however, damage saturation limits do exist [13]. For brittle materials subjected to fatigue loadings, an accurate assessment of the state of damage resulting from the first cycle is important, as this is when the preponderance of damage is accumulated.

During fatigue loading, matrix cracking quickly saturates within the first few cycles and the behavior of the composite is governed by the degradation of the interface [8]. As the constituents debond, energy dissipation associated with frictional sliding occurs. With continued cycling, the interfacial shear strength governing the frictional resistance decreases due to the constituent's wear [14]. Both mechanisms result in an increased material compliance. Moreover, the frictional dissipation results in a looped stress−strain curve (hysteresis) within any given loading and unloading cycle (Fig. 2). The area associated with the hysteresis loop is the energy lost during the corresponding loading and unloading cycle. The frictional resistance within debonded regions affects the energy loss, i.e. the size of the hysteresis loop. Hence, the extent of debonding, as well as the shear strength within these regions are desired. These parameters will be estimated in this study through comparisons of experimental data and numerical predictions from a shear-lag analysis. Understanding the progression of these damage mechanisms on a cycle-by-cycle basis is critical to accurate modeling of the fatigue behavior of

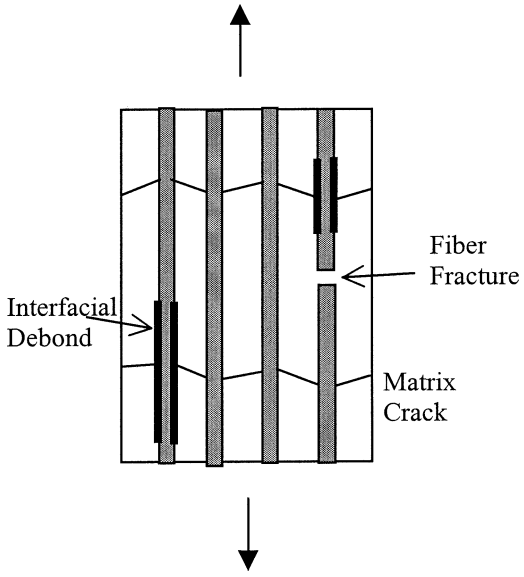

Figure 1. Damage mechanisms associated with a undirectional brittle composite.

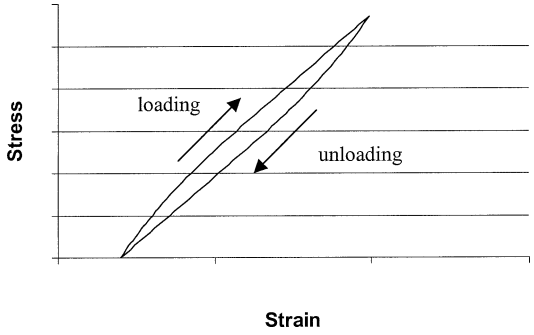

Figure 2. Stress–strain hysteresis resulting from frictional sliding of constituents.

CMCs. Similar analyses have been conducted in the past; however, not for the explicit purpose of determining the progression of the damage modes [5, 8].

2. SHEAR-LAG DEVELOPMENT

The shear-lag approach has proven useful for analyzing CMCs since its introduction by Aveston *et al*. [15]. Its distinct advantage is in reducing a complex stress field containing matrix cracking and fiber/matrix debonding into a simplified one-dimensional analysis. In the present study, the analysis is based upon the shear-lag formulation of Kuo and Chou [16]. The theory simplifies the three-dimensional stress field in the composite by neglecting all but the longitudinal normal (axial or fiber direction) stresses in the constituents, $\sigma_{\mathrm{f}}(x)$ and $\sigma_{\mathrm{m}}(x)$, and the interfacial

Downloaded by [Siauliu University Library] at 07:14 17 February 2013

Downloaded by [Siauliu University Library] at 07:14 17 February 2013

shear stress, $\tau_i(x)$. As indicated, it is also assumed these stresses vary only in the axial direction. The interfacial shear stress is further assumed in the bonded region to be directly proportional to the difference in the average axial displacements of the constituents at any given x-location. In the debonded region, it is assumed equal to a constant frictional shear stress. Relating these assumptions to the equilibrium equations in cylindrical coordinates with the origin taken as the center of the fiber yields the following equations

$$\frac{\mathrm{d}^2\sigma_\mathrm{f}}{\mathrm{d}x^2} - \beta^2\sigma_\mathrm{f} = -\beta^2\sigma_{\mathrm{f_o}}, \tag{1}$$

$$\sigma_\mathrm{m} = \frac{1}{1-v_\mathrm{f}}\left(\sigma - v_\mathrm{f}\sigma_\mathrm{f}\right), \tag{2}$$

$$\frac{\mathrm{d}\sigma_\mathrm{f}}{\mathrm{d}x} = -\frac{2\tau_i}{r_\mathrm{f}}, \tag{3}$$

where v_f is the volume fraction of fibers, r_f is the fiber radius, and σ is the applied composite stress; σ_f, σ_m, and τ_i are the fiber, matrix and interfacial stresses, respectively as determined by the current shear-lag formulation [17]. $\sigma_{\mathrm{f_o}}$ is the fiber

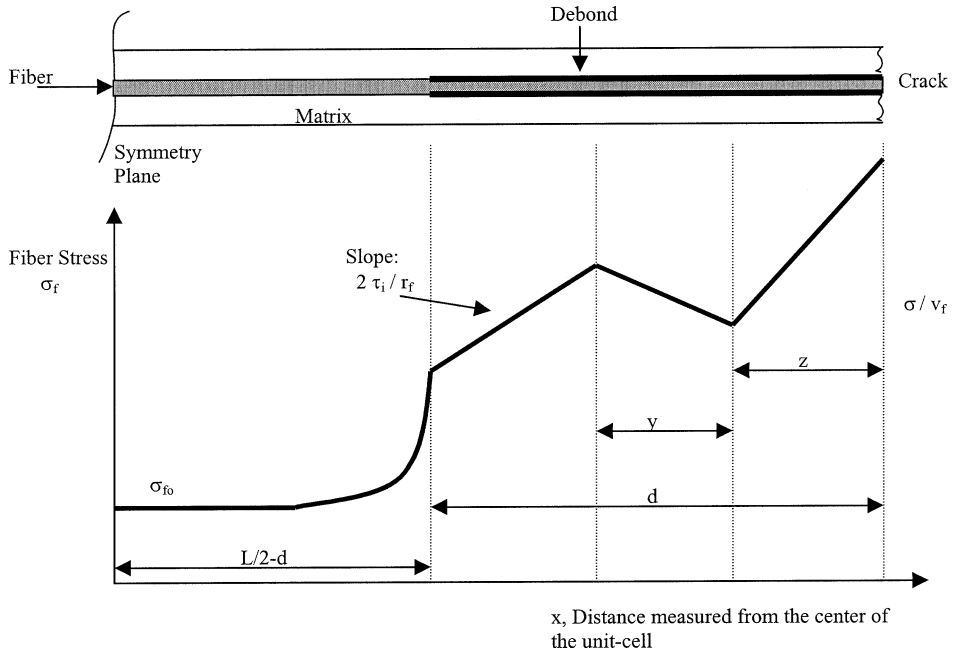

Figure 3. Sketch of assumed fiber stress over one-half of the unit-cell illustrating the effect of interfacial debonding (d), frictional slip during unloading (y), and reloading (z).

stress from the rule of mixtures approximation for an undamaged composite, e.g.

$$\sigma_{f_o} = (E_f/E_1)\sigma + E_f(\alpha_1 - \alpha_f)\Delta T.$$

The parameter β is the shear-lag constant as originally formulated by Kuo and Chou [16].

For CMCs subjected to fatigue loads, the frictional mechanisms inherent in the material produce hysteresis characteristics in the stress–strain response [18]. The shear-lag analysis accounts for this through reverse slip within the interface debond region. Upon load reversal, a reverse slip distance, y, from the matrix crack may be determined by assuming the reverse shear stress is equal in magnitude but opposite in direction from the initial frictional shear stress in the debonded region (Fig. 3). Upon reloading, a counter-reverse slip distance, z, may be determined in a similar manner, and a shakedown analysis ensures for continued cycles. The resulting fiber stress is as indicated in equation (4).

$$\begin{aligned}
\sigma_f(x) &= \sigma_{f_o} + \frac{\cosh(\beta x)}{\cosh(\beta[L/2-d])} \\
&\quad \times \left(\frac{v_m}{v_f}\sigma_{mo} + \frac{2\tau_i}{r_f}\{2(y-z)-d\}\right), \qquad x \in [0, L/2-d] \\
\sigma_f(x) &= \frac{\sigma}{v_f} + \frac{2\tau_i}{r_f}[x + 2(y-z) - L/2], \qquad x \in [L/2-d, L/2-y] \\
\sigma_f(x) &= \frac{\sigma}{v_f} + \frac{2\tau_i}{r_f}[L/2 - 2z - x], \qquad x \in [L/2-y, L/2-z] \\
\sigma_f(x) &= \frac{\sigma}{v_f} + \frac{2\tau_i}{r_f}[L/2 - x], \qquad x \in [L/2-z, L/2],
\end{aligned} \tag{4}$$

where d, y and z denote the debond, reverse slip and counter-reverse slip lengths, respectively (as illustrated in Fig. 3).

For the present analysis, once the fiber stress distribution is know, the composite strain may be determined since it is assumed equal to the average strain in the fiber, i.e.

$$\varepsilon_c = \frac{1}{E_f L}\int_L \sigma_f(x)\,dx + (\alpha_f - \alpha_c)\Delta T. \tag{5}$$

3. INTERFACIAL BEHAVIOR DURING FATIGUE

Due to the inherent brittleness of ceramic materials, matrix cracking usually arrests after the first few loading cycles during constant amplitude fatigue tests. Mechanisms associated with oxidation, fatigue crack growth and the like which might lend themselves to continued matrix failure are not considered in the present study [19]. Furthermore, for this particular study, fiber failure is also not considered. As a result, changes in the laminate behavior, during subsequent loading cycles,

Downloaded by [Siauliu University Library] at 07:14 17 February 2013

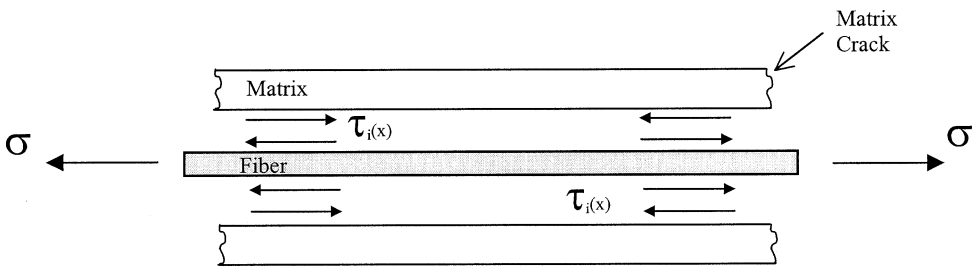

Figure 4. Interfacial shear stress governs load transfer between constituents. Within bonded regions, the shear is large due to molecular bonding. In debonded regions, friction governs shear. The frictional shear decreases as constituents wear.

Downloaded by [Siauliu University Library] at 07:14 17 February 2013

are attributed solely to the degradation of the fiber/matrix interface. In particular, load transfer between the constituents is compromised through debonding, in conjunction with the degeneration in the frictional resistance between the two media [equation (3)].

Initially, constituent load transfer is high due to strong chemical binding; however, with debonding, the shear stress, $\tau_i(x)$, notably declines since it is assumed to be governed solely by Coulomb friction within failed regions (Fig. 4). Moreover, with frictional sliding occurring in debonded regions, the shear resistance declines as the constituents wear during fatigue.

4. HYSTERETIC ENERGY LOSSES (EXPERIMENTAL)

Energy losses associated with frictional sliding in debond regions manifests as closed hysteresis loops in the laminate's stress–strain response (Fig. 2). The size, shape, and location of each cyclic loop are indicative of the amount of damage within the composite. Specifically, the area associated with the hysteresis loop represents the energy (strain energy per volume) dissipated during each loading and unloading cycle.

For the current study, the experimental stress–strain data were tests presented by Evans *et al*., for a unidirectional SiC/CAS laminate subjected to room-temperature fatigue [6]. The material response during cycles 1, 5, 9 and 109 are illustrated in Fig. 5. The strain energies associated with these cycles are provided in Table 1.

As the data in Table 1 indicate, the energy dissipated increases initially during cycling. This corresponds with the formation of microstructural damage. As the virgin specimen is loaded, matrix cracks initiate, fibers fail, and interface bonds are broken. The damage formation, as well as the constituent sliding which is now permitted, accounts for the increased hysteresis and material compliance. As stated previously, matrix and fiber damage saturates early on and then growth of dissipated energy is attributed to interfacial mechanics. Eventually, as the constituents completely debond and wear, the hysteresis loops once again collapse or reduce (i.e. loading and unloading curves coincide) since the now smooth surfaces flow freely over one another.

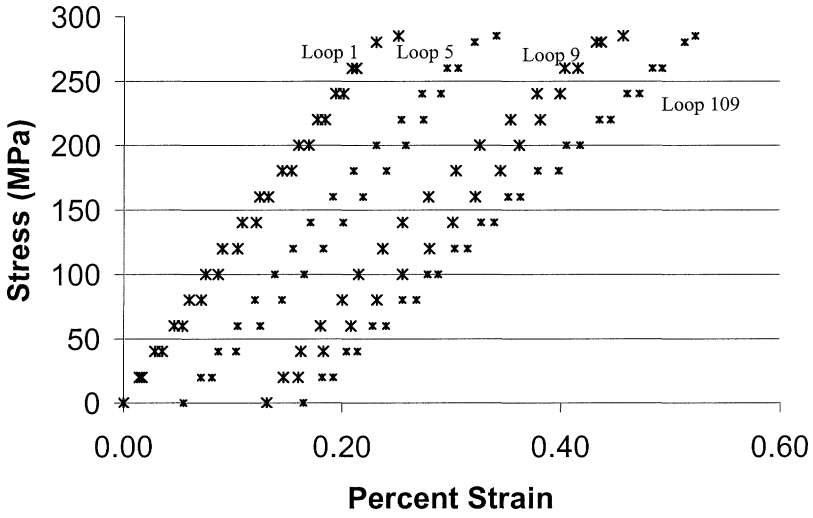

Figure 5. Experimental data estimated from Evans *et al*. [6].

Table 1.
Strain energy from experimental data [6]

Loading cycle	Strain energy (kJ/m^3)
1	22
5	55
9	80
109	30

From the data presented in Fig. 5, it is clear that over the first 9 cycles the energy dissipated with each cycle continues to increase. However, by cycle 109, the hysteresis loop has collapsed significantly, i.e. energy loss is almost negligible.

5. HYSTERETIC ENERGY LOSSES (COMPUTATIONAL)

The current theory, expressed in equations (4) and (5), permits generation of composite stress–strain behavior and therefore estimates of energy loss per cycle based upon the extent of interfacial debonding, d, and the magnitude of the interfacial shear, τ_i. The matrix crack density is assumed measurable and fixed upon completion of the first load cycle. The remaining parameters are material constants as given in Table 2.

Graphs illustrating the energy loss per cycle as a function of sliding stress (for a given debond length) were generated to compare the theoretical and empirical results. Figure 6 illustrates the theoretical energy loss (as a function of sliding stress) for a completely debonded interface and crack density of 8/mm [16].

Downloaded by [Siauliu University Library] at 07:14 17 February 2013

Table 2.
Material property data [20]

E_f	210 GPa	E_m	95.5 GPa
α_f	3.10 μ/°C	α_m	4.50 μ/°C
G_f	65.0 GPa	G_m	28.0 GPa
ΔT	−1000°C	r_f	7.50 μm
Crack Density	8/mm	v_f	0.38
τ_i	5 MPa	Min Stress	0
Max Stress	285 MPa	% debond (1st loop)	25.0
% debond (2nd loop)	50.0	% debond (3rd loop)	75.0

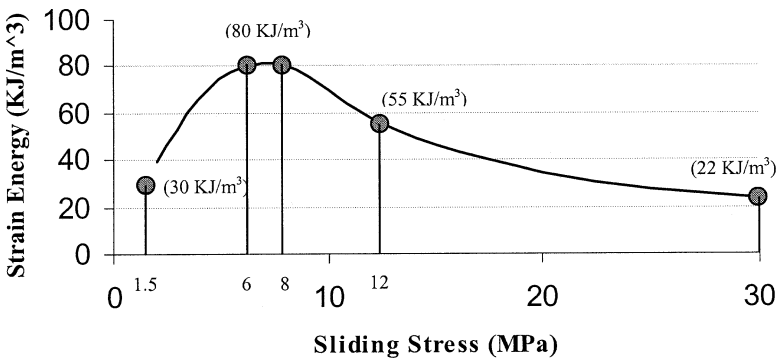

Figure 6. Energy dissipated as a function of interfacial shear stress. Results shown assume a completed debonded interface and crack density of 8/mm.

Table 3.
Estimate of shear degradation (per cycle) assuming complete debonding

Loading cycle	Magnitude of shear (MPa)
1	30
5	12
9	6 or 8
109	1.5

Estimates for the interfacial shear stress (per cycle) may now be obtained through comparison of the experimental data in Table 1 with the computational results illustrated in Fig. 6. The predicted degradation in shear is provided in Table 3. These results shown assume that the interface in completely debonded prior to any loading.

Note that due to the 'hump' in the energy curve illustrated in Fig. 6, a unique solution for the shear stress during cycle 9 does not exist. Theoretical predictions of $\tau_i = 6$ MPa and 8 MPa both correspond to 80 kJ/m^3. This problem can, in some cases, be overcome by imposing necessary physical constraints. For example, the constituents are not permitted to re-bond, and hence, the assumed debond

Downloaded by [Siauliu University Library] at 07:14 17 February 2013

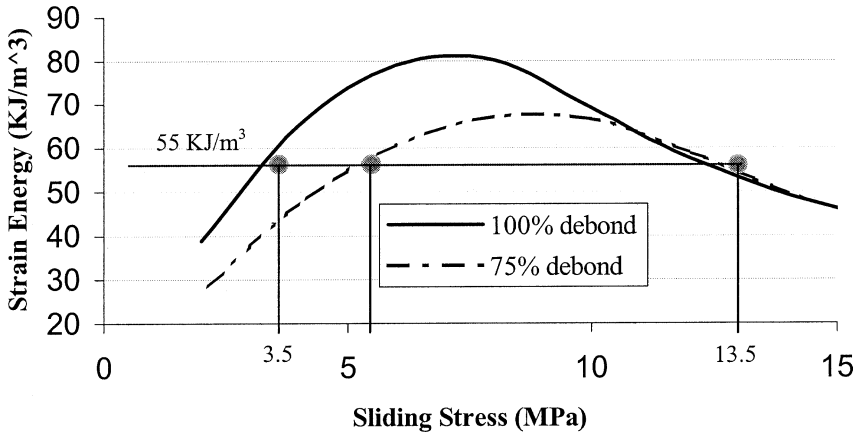

Figure 7. Energy dissipated as a function of interfacial shear stress.

Table 4.
Initially valid solutions for cycle 5 considering only 75 and 100% debonding. Cases 1 and 3 are shown to be invalid when physical constraints are imposed

Case 1		Case 2		Case 3		Case 4	
Debond	Shear	Debond	Shear	Debond	Shear	Debond	Shear
75%	5 MPa	75%	13.5 MPa	100%	3.5 MPa	100%	13.5 MPa

length may only grow. In addition, the magnitude of the interfacial shear stress is necessarily prevented from increasing with wear. Alternatively, one may be able to differentiate between the possible solutions by imposing conditions associated with one of the myriad of micromechanics models that have been presented in the literature. Clearly, if the stress distribution between the two matrix cracks is 'known' and applied to predict the extent of debonding, then delineation between the possible solutions is not necessary. However, this is exactly the type of analysis that the present study attempts to avoid.

As an example, use the present theory to try to predict the extent of debonding and interfacial shear corresponding to the 5th cycle of experimental data (55 kJ/m^3). For argument sake, assume that, as illustrated in Fig. 7, the interface is permitted to be only either 75 or 100% debonded. In this case, there initially exist four solutions for cycle 5 (Table 4).

However, upon considering the physical constraint that the shear may only degrade and considering the results presented in Table 3 for cycle 9, cases 1 and 3 are eliminated as valid solutions since the shear stress is required to be greater than 6 MPa. Moreover, it may now also be concluded that the amount of debonding at (and beyond) the 9th cycle is greater than 75%.

Finally, consider the energy loss as a function of sliding stress for a wider range of debonding, specifically 25, 50, 75 and 100% debonded interface (Fig. 8).

Downloaded by [Siauliu University Library] at 07:14 17 February 2013

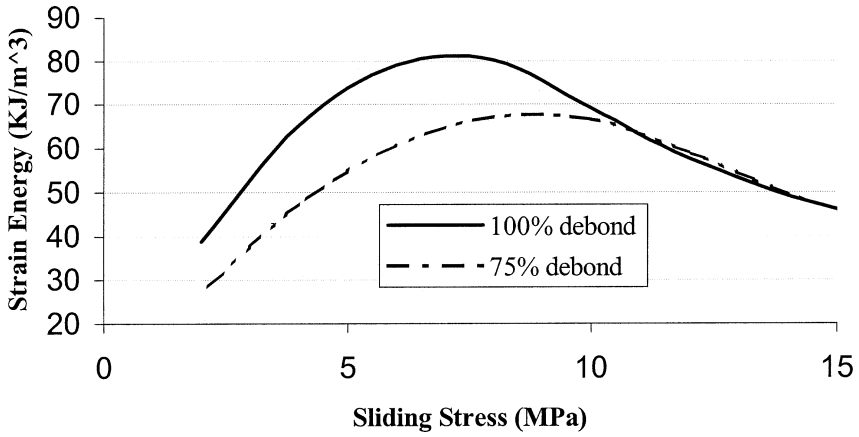

Figure 8. Dissipation for four states of debonding.

Furthermore, for purposes of analysis, assume that these are the only valid states of debonding and that the progression begins at 25% after the first cycle.

In this case, based upon the information provided in Fig. 8, several conclusions may be drawn as to both the progression of interfacial debonding and the degradation of the interfacial shear stress. First, over the assumed cyclic range (1 to 109 cycles), the interfacial shear stress degrades from 12 MPa to 1.5 MPa. Moreover, the interface must be completed debonded by the 5th cycle since, as previously argued, in order to satisfy the imposed physical constraints the amount of debonding must be greater that 75% and is therefore assumed completed debonded. Cases 1 and 2 in Table 4 are invalidated by the requirement that the shear cannot increase with cycling. As a result, the interfacial shear is known exactly after the 9th cycle, i.e. case 4 in Table 4.

As the above procedure is generalized to relax the debonding constraint, as well as to consider an expanded set of experimental data, the analysis and reduction of data clearly become more involved. However, the procedure shown in this study remains a viable approach for inferring the degradation of the interface and thereby providing a more accurate means of modeling the fatigue behavior of CMCs. In addition, the predictions made in the paper were based solely on the hysteretic energy loss. Similar analyses could be conducted considering modulus degradation, residual strain and S-N behavior, and invalid solutions could be eliminated through comparing these data much in the same manner, i.e. by imposing physical constraints.

6. CONCLUSIONS

Knowledge of the condition of fiber/matrix interface is critical in composite modeling. Unfortunately, with ceramic matrix composites (CMCs), little is known about the specific progression of interfacial damage during fatigue loading. What

Downloaded by [Siauliu University Library] at 07:14 17 February 2013

is known is that during cycling the constituents debond, slide against one another, and wear occurs, leading to a decline in the magnitude of the shear stress between the fiber and matrix. Both of these mechanisms, constituent debonding and the degradation in shear, govern in large part the mechanical behavior (stress–strain response) and ultimately the residual strength, stiffness and life of the laminate. Matrix failure has little to do with the progression of the latter since saturation occurs early on due to the inherent nature of the brittle ceramic. Moreover, in CMCs, the extent of matrix cracking can be measured (experimentally) whereas the extent of debonding and the instantaneous shear stress cannot. Traditional 'push-in' or 'pull-out' tests fail to provide specific evidence of the *in-situ* behavior during mechanical fatigue [21].

This study proposes a means of inferring the state of the interface through comparison of experiment and theoretical hysteretic energy loss on a cycle by cycle bases. In the past, estimates for the shear degradation have been conducted in a similar manner; however, the interface is typically assumed to be completely debonded [8] or governed by some simplistic failure criteria (e.g. maximum shear stress criterion) [22]. With the current technique, neither approach is required. Moreover, several 'shear degradation functions' have been proposed in the literature [6, 18, 23] and the present theory provides a means for comparison.

As a first step, a limited number of solution sets have been considered in this paper. Further generalization of the theory should provide greater insight into the progression of interfacial damage. Since, for any given loading cycle, the theory can yield multiple solutions, e.g. theoretical predictions with debond length and interfacial shear strength $(d, \tau_i) = (75\%, 5\ \text{MPa})$ and $(d, \tau_i) = (100\%, 13.5\ \text{MPa})$ may yield identical strain energy losses ($55\ \text{kJ/m}^3$), it is necessary to impose physical constraints, such as the constituent cannot re-bond, in order to eliminate unrealistic solutions. Moreover, similar comparisons of experimental and theoretical data based upon modulus degradation, residual strain progression and S-N behavior should provide further evidence as to the nature of the specific progression of the two parameters (i.e. debond length and interfacial shear strength). Finally, the fact that of our results agree well with similar data published in the literature not only lends credence to the approach, but also illustrates the utility of using simplified models to validate more rigorous theory.

Acknowledgement

The authors would like to thank the Air Force Office of Scientific Research for the support of this study.

REFERENCES

1. T. A. Parthasarathy, D. B. Marshall and R. J. Kerans, Analysis of the effect of interfacial roughness on fiber debonding an sliding in brittle matrix composites, *Acta Metallurgica et Materialia* **42** (11), 3773–3784 (1994).

Downloaded by [Siauliu University Library] at 07:14 17 February 2013

Downloaded by [Siauliu University Library] at 07:14 17 February 2013

2. P. D. Jero, R. J. Kerans and T. A. Parthasarathy, Effect of interfacial roughness on interfacial roughness of the frictional stress measured using push-out tests, *J. Amer. Ceram. Soc.* **74** (11), 2793 (1991).
3. F. Rebaillat, J. Lamon and A. G. Evans, A microcomposite test procedure for evaluating the interface properties of ceramic matrix composites, *J. Amer. Ceram. Soc.* **78** (2), 401–405 (1995).
4. J. M. Domergue, E. Vagaggini and A. G. Evans, Relationships between hysteresis measurements and constituent properties of ceramic matrix composites: I, Theory, *J. Amer. Ceram. Soc.* **78** (10), 2709–2720 (1995).
5. J. M. Domergue, E. Vagaggini and A. G. Evans, Relationships between hysteresis measurements and constituent properties of ceramic matrix composites: II, Experimental studies on unidirectional materials, *J. Amer. Ceram. Soc.* **78** (10), 2721–2731 (1995).
6. A. G. Evans, F. W. Zok and R. M. McMeeking, Fatigue of ceramic matrix composites, *Acta Metallurgica et Materialia* **43** (3), 859–875 (1995).
7. F. Hild, A. Burr and F. Leckie, Matrix cracking and debonding of ceramic matrix composites, *Intern. J. Solids and Structures* **33** (8), 1209–1220 (1996).
8. A. W. Pryce and P. A. Smith, Matrix cracking in unidirectional ceramic matrix composites under quasi-static and cyclic loading, *Acta Metallurgica et Materialia* **41** (4), 1269–1281 (1993).
9. H. K. Bowen, Advanced ceramics, *J. Amer. Ceram. Soc.* **73** (2), 169–176 (1990).
10. T. Kotil, J. W. Holmes and M. Camninou, Origin of hysteresis observed during fatigue of ceramic-matrix composites, *J. Amer. Ceram. Soc.* **73** (7), 1879–1883 (1990).
11. A. G. Evans, J. M. Domerque and E. Vagaggini, Methodology for relating the tensile constitutive behavior of ceramics-matrix composites to constituent properties, *J. Amer. Ceram. Soc.* **77**, 1425–1435 (1995).
12. A. G. Evans, Perspective on the development of high-toughness ceramics, *J. Amer. Ceram. Soc.* **73** (2), 187–206 (1990).
13. M. E. Walter and G. Ravichandran, An experimental investigation of damage evolution in a ceramic matrix composite, *J. Engng Mater. Technol.* **117**, 101–107 (1995).
14. J. W. Holmes and C. Cho, Experimental observations of frictional heating in fiber-reinforced composites, *J. Amer. Ceram. Soc.* **74** (4), 929–938 (1992).
15. J. Aveston, G. A. Cooper and A. Kelly, Single and multiple fracture; the properties of fiber composites, in: *Conf. Proc.*, pp. 15–26. National Physical Laboratory, IPC Science and Technology Press, Guildford, UK (1971).
16. W. S. Kuo and T. W. Chou, Multiple cracking of unidirectional and cross-ply ceramic matrix composites, *J. Amer. Ceram. Soc.* **78** (3), 745–755 (1995).
17. J. P. Solti, S. Mall and D. D. Robertson, Modeling damage in unidirectional ceramic matrix composites, *Compos. Sci. Technol.* **54**, 55–66 (1995).
18. J. P. Solti, S. Mall and D. D. Robertson, A simplified approach for modeling fatigue in unidirectional ceramic matrix composites, *J. Compos. Technol. and Research* **18** (3), 167–178 (1996).
19. R. Talreja, Fatigue of fibre-reinforced ceramics, in: *Proc. 11th Risø International Symposium on Metallurgy and Materials Science: Structural Ceramics — Processing, Microstructure, and Properties*, pp. 145–159. Risø National Laboratory, Roskilde, Denmark (1990).
20. W. S. Kuo, Damage of multi-directionally reinforced ceramic matrix composites. PhD thesis, Department of Mechanical Engineering, University of Delaware (1992).
21. R. N. Singh, Influence of interfacial shear stress on first matrix cracking stress in ceramic matrix composites, *J. Amer. Ceram. Soc.* **72**, 2930–2937 (1990).
22. I. M. Daniel, G. Anastassopoulos and J. W. Lee, Failure mechanisms and interfacial shear strength in brittle-matrix composites, in: *Advances in Experimental Mechanics and Biomimetics*, W. F. Jones (Ed.), pp. 57–69. American Society of Mechanical Engineers, New York, NY (1992).

23. D. Rouby and P. Reynaud, Fatigue behavior related to interface modification during load cycling in ceramic-matrix fibre composites, *Compos. Sci. Technol*. **48**, 109–118 (1993).

Downloaded by [Siauliu University Library] at 07:14 17 February 2013